*J. Fluid Mech.* (1997), *vol.* 346, *pp.* 181–200. Printed in the United Kingdom



# Global capillary instability of an inclined jet

By P. A. YAKUBENKO

Department of Hydraulic Engineering, The Royal Institute of Technology,
100 44 Stockholm, Sweden

(Received 28 August 1995 and in revised form 21 April 1997)

The primary goal of the paper is to demonstrate that a circular jet of inviscid liquid, which issues from a nozzle at an angle to the gravitational field, can sustain a self-excited linear global mode. The mode is found for the flow that is locally convectively unstable at every point, i.e. has no region of local absolute instability. A simple experiment shows that the mode can evolve into a wave of finite amplitude, which is localized in space near the nozzle.

Section 2 of the paper summarizes some recent developments in the linear theory of stability of weakly inhomogeneous flows.

## 1. Introduction

The linear stability analysis of a stationary flow is usually based on the hypothesis that the time-dependence of a small disturbance has the form $\exp(-\mathrm{i}\omega t)$. The study of the disturbance evolution is then reduced to the study of a boundary-value problem for a system of linear differential equations. If the basic flow has either a finite length in the streamwise direction or is inhomogeneous, the streamwise direction is also an 'eigenvalue direction'. The flow is called globally unstable if the eigenfunction or global mode exists for at least one eigenfrequency $\omega$ with a positive imaginary part. The term *global instability* was introduced by Kulikovskii (1966) to describe instabilities in homogeneous flows of large but finite length (see also Lifshitz & Pitaevskii 1981; Bers 1983). The term contrasts with *boundary instability*, which is an instability associated with one of the streamwise boundaries. More recently, the term was used for the description of instabilities in weakly inhomogeneous flows (Pierrehumbert 1984; Kulikovskii 1985; Monkewitz, Huerre & Redekopp 1987; Chomaz, Huerre & Redekopp 1988). The usage is in contrast to the concept of *local instability* that is a property of some fictitious homogeneous flow corresponding to the given fixed value of the streamwise coordinate. More details can be found in §2 of the present paper.

The capillary instability of an infinitely long jet with respect to temporally growing disturbances was analysed by Rayleigh (1878). An inviscid jet is unstable with respect to any axially symmetric disturbance if the wavelength is greater than the perimeter of the jet cross-section. Keller, Rubinow & Tu (1973) analysed the capillary instability of a circular jet with respect to spatially growing disturbances. (A summary of the results can be also found in the reviews by Bogy 1979 and Ashgriz & Mashayek 1995.) The absolute and convective types of instability of a circular cylindrical jet with respect to axially symmetric disturbances were investigated analytically by Leib & Goldstein (1986*a*), Monkewitz (1990), and experimentally by Monkewitz *et al.* (1988). They have found that the Weber number used to distinguish absolute from convective instability depends on the shape of the axial velocity profile of the basic

flow. A change in the effective value of the surface tension can also be achieved by the inertia of the surrounding medium and the liquid viscosity if they are taken into account (Leib & Goldstein 1986*b*; Lin & Lian 1989; Monkewitz 1990).

Global instability of a homogeneous jet of large but finite length was analysed by Yakubenko (1997). The flow can be globally unstable even if the corresponding infinitely long jet is convectively unstable. Global instability of a jet that flows downward from a nozzle has been discussed by Monkewitz (1990) and Le Dizès (1996). The global instability is caused by a region of local absolute instability, which can appear near the nozzle. In the present paper, a global instability analysis is performed for an inclined circular jet that has no region of local absolute instability.

## 2. Global modes in weakly inhomogeneous flows

The streamwise spatial development of the basic flow can be characterized by a length scale $L$, and the local instability can be characterized by a typical wavelength $\lambda$. The parameter $\varepsilon = \lambda/L$ is a measure of the spatial inhomogeneity of the flow in terms of the disturbance propagation. If $\varepsilon \ll 1$, the basic flow depends only on the slow streamwise coordinate $X = \varepsilon x$ and is usually called weakly inhomogeneous.

Any global mode of frequency $\omega$ can be asymptotically represented when $\varepsilon \to 0$ by

$$\sum_{q=0}^{\infty} \left\{ \sum_{p} C_p \left[ \varepsilon^q A_{p,q}(X, r; \omega) \right] \exp\left[ \mathrm{i}\varepsilon^{-1} \int_{X_p}^{X} k_p(\omega, \xi)\, \mathrm{d}\xi \right] \right\}, \tag{2.1}$$

in which $C_p$ are arbitrary constants, and branches $k_p(\omega, X)$ of the local wavenumber are found from the local dispersion relation

$$D(k, \omega; X) = 0.$$

For each value of $p$, functions $A_{p,q}(X, r; \omega)$ can be computed recursively up to any $q$.

The first term in the series (2.1)

$$\sum_{p} C_p A_{p,0}(X, r; \omega) \exp\left[ \mathrm{i}\varepsilon^{-1} \int_{X_p}^{X} k_p(\omega, \xi)\, \mathrm{d}\xi \right] \tag{2.2}$$

is usually called the WKBJ approximation. The foregoing approach originates from quantum mechanics. It was adapted for stability investigations by Silin (1963) and Krall & Rosenbluth (1963) in plasma physics. More recently, it was used in fluid dynamics (e.g. Drazin 1974; Crighton & Gaster 1976).

In the general case, no single expression of form (2.2) approximates the solution for the entire real $X$-axis (or complex $X$-plane). Thus, the approximation fails in the neighbourhood of the so-called turning points $X_{m,n}$ that are solutions of the equation

$$k_m(\omega, X) = k_n(\omega, X), \tag{2.3}$$

in which $\omega$ is a parameter. However, the approximation can be composed of several different linear combinations of form (2.2) at different domains of the complex $X$-plane.

We will refer to the lines defined from

$$\mathrm{Im}\left\{ \int_{X_{m,n}}^{X} [k_m(\omega, \xi) - k_n(\omega, \xi)]\, \mathrm{d}\xi \right\} = 0,$$

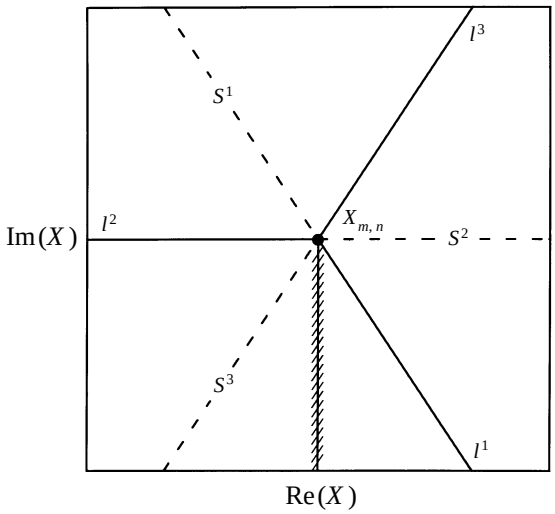


FIGURE 1. Solid and dashed lines are Stokes and anti-Stokes lines, respectively. The branch cut is shown by the hatched line.

in which $\omega$ is a parameter, as the *Stokes lines*, and from

$$\mathrm{Re}\left\{\int_{X_{m,n}}^{X}\left[k_m(\omega,\xi)-k_n(\omega,\xi)\right]\mathrm{d}\xi\right\}=0$$

as the *anti-Stokes lines*. These names are often used vice versa (e.g. Heading 1962; Meyer 1989). The present order is typical for modern fluid dynamics (e.g. Huerre & Monkewitz 1990; Le Dizès *et al.* 1996).

Let $X_{m,n}$ be a single turning point, i.e. a single root of (2.3). Then, three Stokes lines emerge from it (see figure 1). The lines locally split the complex $X$-plane into three sectors. The bisectrix of each sector is the anti-Stokes line. The solution

$$K_m = A_{m,0}(X,r;\omega)\exp\left[\mathrm{i}\varepsilon^{-1}\int_{X_{m,n}}^{X}k_m(\omega,\xi)\,\mathrm{d}\xi\right]$$

is called dominant (in sector $S^j$) if it is exponentially large with respect to $K_n$, the latter then being called subdominant. (The maximum domination is reached at the anti-Stokes line inside $S^j$.) At the Stokes lines, both solutions are of the same order of magnitude.

Let $K_m$ be dominant in sector $S^1$, and the global mode be approximated by

$$C_mK_m + C_nK_n, \tag{2.4}$$

at the Stokes line $l^2$ (see figure 1). If the solution is formally continued from $l^2$ into the sector $S^1$, the term $C_nK_n$ may become small compared to the truncated part of the series (2.1). Strictly speaking, any value could be prescribed then to the coefficient $C_n$ inside $S^1$. However, at the line $l^3$, both solutions again have the same order of magnitude. Moreover, in sector $S^2$, solution $K_n$ is dominant.

In order to construct an approximation that is valid in all three sectors, Stokes (1857) suggested the following procedure. As the approximation (2.4) is continued from $l^2$ to $l^3$ through sector $S^1$, coefficient $C_m$ remains unchanged, while $C_n$ changes to $C_n + TC_m$, in which $T$ is called the Stokes constant.

In the above example, $T = -\mathrm{i}$. In the general case, the value of $T$ depends on the type of turning point; its magnitude is typically of order unity. If the approximation is continued around the turning point in the opposite direction, $T$ changes to $-T$. Note that $C_n$ remains unchanged if $C_m = 0$, i.e. if only a subdominant solution must be used in $S^1$ for some reason.

The jump in the coefficient at the subdominant solution is often called the Stokes phenomenon. Stokes (1857) found that the jump must occur at the anti-Stokes line inside the sector if one wants to compute the series (2.1) with maximum accuracy. Since the WKBJ approximation takes into account only the first term in the series, the jump could actually be performed at any line inside the sector. However, the anti-Stokes line is usually chosen for convenience.

If $k(\omega, X)$ has more than two branches, several sets of the Stokes and anti-Stokes lines can exist. The sets are independent. Thus, the lines from different sets may intersect at any point and even coincide, yet the lines belonging to the same set may intersect only at turning points. (A procedure that helps to locate the lines is discussed in the Appendix.)

Hence, the complex $X$-plane is divided by the network of anti-Stokes lines into domains where the global mode may be approximated by different linear combinations of elementary WKBJ solutions. If the real $X$-axis crosses the boundaries of these domains, it is divided into segments. Linear Stokes relations link the coefficients at the elementary WKBJ solutions for each pair of the consequent segments. Thus, the ends of the segments can be considered as points (within the flow) at which boundary conditions are specified. We will refer to them as *points of inner reflection.*

Hence, the global mode is a sequence of linear combinations of the elementary WKBJ solutions. The combinations are connected by the physical boundary conditions on the streamwise boundaries of the flow and by the additional boundary conditions that are the Stokes relations at the points at which the real $X$-axis crosses the anti-Stokes lines.

Let us introduce the following notations:

$$K_n^\alpha \equiv A_{n,0}(X, r; \omega) \exp\left[\mathrm{i}\varepsilon^{-1} \int_{X^\alpha}^{X} k_n(\omega, \xi)\, \mathrm{d}\xi\right],$$

$$Q_n^{\alpha,\beta} \equiv \exp\left[\mathrm{i}\varepsilon^{-1} \int_{X^\alpha}^{X^\beta} k_n(\omega, \xi)\, \mathrm{d}\xi\right].$$

We will refer to $K_n^\alpha$ as an *elementary WKBJ wave* propagating from $X = X^\alpha$, and to $Q_n^{\alpha,\beta}$ as a *spatial amplification coefficient* of the wave $K_n^\alpha$ at the interval $[X^\alpha, X^\beta]$.

If the flow model satisfies causality, a constant $M \geqslant 0$ exists such that for $\mathrm{Im}(\omega) > M$, one has $\mathrm{Im}[k_p(\omega, X)] \neq 0$ for every $p$ and any value of $X$. Thus, all branches of the local wavenumber can be split into two groups according to the signs of their imaginary parts for $\mathrm{Im}(\omega) > M$. The waves corresponding to the branches with positive and negative imaginary parts propagate to the right and to the left, respectively. For any frequency $\omega$ with $\mathrm{Im}(\omega) > M$, every wave is spatially damped in its direction of propagation.

At each boundary point $X = X^\beta$, the boundary conditions can be expressed in the following form:

$$C_m^\beta = \sum_n P_{n,m}^\beta Q_n^{\alpha,\beta} C_n^\alpha, \tag{2.5}$$

in which $P_{n,m}^\beta$ is referred to as the *conversion coefficient* for the incoming wave $K_n$

and the outgoing wave $K_m$ at the point $X = X^\beta$. At the physical boundaries of the flow, the conversion coefficients are typically of order unity and independent of the frequency $\omega$. At the points of inner reflection, they can be calculated as follows.

Let $X^\beta$ be a point where the real $X$-axis crosses the anti-Stokes line that emerges from the turning point $X_{m,n}$ that corresponds to the branches $k_m(\omega, X)$ and $k_n(\omega, X)$. If the solution $K_m$ is dominant at the line, then $P^\beta_{j,j} = 1$ for any $j$ and $P^\beta_{j,i} = 0$ for any $i \neq j$ except

$$P^\beta_{m,n} = T R^\beta_{m,n},$$

in which $T$ is the Stokes constant associated with the turning point $X_{m,n}$, and

$$R^\beta_{m,n} = \exp\left\{ \mathrm{i}\varepsilon^{-1} \int_{X^\beta}^{X_{m,n}} [k_m(\omega, \xi) - k_n(\omega, \xi)]\, \mathrm{d}\xi \right\}. \tag{2.6}$$

Since the integration in (2.6) is performed along the anti-Stokes line, the equation can be rewritten as

$$R^\beta_{m,n} = \exp\left\{ -\varepsilon^{-1} \mathrm{Im} \int_{X^\beta}^{X_{m,n}} [k_m(\omega, \xi) - k_n(\omega, \xi)]\, \mathrm{d}\xi \right\}.$$

If the turning point $X_{m,n}$ is located at the real $X$-axis, i.e. if $X^\beta$ coincides with $X_{m,n}$, then $R^\beta_{m,n} = 1$. If the distance between $X^\beta$ and $X_{m,n}$ is large, then $\left|R^\beta_{m,n}\right| \ll 1$ so that $\left|P^\beta_{m,n}\right| \ll 1$. Hence, the wave interaction caused by turning points that are located far away from the real axis is weak and often can be neglected.

The following frequency selection criterion for the global modes has been obtained by Kulikovskii (1985). If for some frequency $\omega^*$, there exists a cyclic sequence of elementary WKBJ waves $K_{m_1}, ..., K_{m_N}$ that are consequently converted from one to another at points $X^1, ..., X^N$, and the total product of their space amplification coefficients and their conversion coefficients equals unity, i.e.

$$\prod_{j=1}^{N-1} \left[ Q^{j,j+1}_{m_j}(\omega^*)\, P^{j+1}_{m_j,m_{j+1}}(\omega^*) \right] Q^{N,1}_{m_N}(\omega^*)\, P^{1}_{m_N,m_1}(\omega^*) = 1, \tag{2.7}$$

then there exists a global frequency

$$\omega = \omega^* + O(\varepsilon).$$

In particular, the flow is globally unstable if $\mathrm{Im}(\omega^*)$ is positive and sufficiently large. At least two points among $X^1, ..., X^N$ must be different. The numbers $m_1, ..., m_N$ are not necessarily all different, yet at least two of them must be different, since a cyclic sequence involves at least two waves that propagate in opposite directions. The sequence forms a 'skeleton' of the global mode; it may involve a part of those elementary waves that form the global mode. For instance, the typical situation for infinite and semi-infinite flows is that some waves propagate to infinity without interacting with the other ones.

For homogeneous flows of large but finite length, the global mode is based on a pair of waves that are enclosed between the flow boundaries. The frequency selection criterion (2.7) takes the following simple form (Kulikovskii 1966):

$$\min_m \left\{ \mathrm{Im}\left[k_m(\omega^*)\right] \right\} = \max_n \left\{ \mathrm{Im}\left[k_n(\omega^*)\right] \right\},$$

in which the minimum and maximum are taken among the waves propagating to the right and left, respectively. Absolute instability is sufficient but not necessary for the flow to be globally instable (e.g. Yakubenko 1997).

In many cases of weakly inhomogeneous flows, the global mode can be based on a pair of waves that propagate in opposite directions. For semi-infinite flows, the waves are enclosed between the boundary and a point of inner reflection (e.g. Monkewitz, Huerre & Chomaz 1993). For double-infinite flows, they are enclosed between two points of inner reflection. The global frequencies can then be found from the so-called quantization relation (Silin 1963; Le Dizès *et al.* 1996)

$$\frac{1}{2\varepsilon}\int_{X^1}^{X^2}\left[k_m\left(\omega^*,\xi\right)-k_n\left(\omega^*,\xi\right)\right]\mathrm{d}\xi=\pi(l+\tfrac{1}{2}),$$

in which $l$ is an arbitrary integer, and the integration is performed in the complex $X$-plane between two turning points $X^1$ and $X^2$. However, the proper choice of the points still requires the investigation of the topological structure of the Stokes lines. The investigation can be a difficult task even for a second-order differential equation (Dnestrovskii & Kostomarov 1964; Le Dizès *et al.* 1996). However, some of the global frequencies can often be found by making use of the local properties of the system. One can define the *local absolute frequency* $\omega_0(X)$ that has the maximal imaginary part among solutions of the equation

$$k_m(\omega,X)=k_n(\omega,X),$$

in which $X$ is a parameter. (Additionally, the waves $K_m$ and $K_n$ must propagate in opposite directions, e.g. Bers 1983.) One of the global frequencies is approximately $\omega_0(X_s)$, in which $X_s$ is a saddle point of the local absolute frequency, i.e. a solution of the equation

$$\frac{\mathrm{d}\omega_0}{\mathrm{d}X}(X)=0, \tag{2.8}$$

such that $\mathrm{Im}\left[\mathrm{d}^2\omega_0/\mathrm{d}X^2(X_s)\right]<0$ (Chomaz, Huerre & Redekopp 1991). The flow is then globally unstable if $\mathrm{Im}\left[\omega_0(X_s)\right]>0$, which implies that the flow has a region of local absolute instability. (This region must be actually larger than some arbitrary size.) In the general case, the presence of a local absolute instability region is a necessary but not sufficient condition for instability of global modes associated with saddle points of the local absolute frequency (Huerre & Monkewitz 1990; Chomaz *et al.* 1991; Hunt & Crighton 1991). Equation (2.8) can be rewritten as

$$\frac{\partial\omega}{\partial k}(k_s,X_s)=\frac{\partial\omega}{\partial X}(k_s,X_s)=0.$$

The simultaneous saddle point of the local frequency $\omega(k,X)$ on the complex $k$- and $X$-planes is a stationary point of the complex Hamilton equations that represent the disturbance evolution as a trajectory in the $(k,X)$ complex space (Iordanskii 1988).

The existence of the unstable global modes based on a sequence of more than two elementary WKBJ waves has no relation at all to the local absolute/convective instability of the flow under consideration. For example, a globally unstable system that is double-infinite and locally convectively unstable has been found by Kulikovskii (1993) in his studies of the transverse oscillations of an elastic tube conveying fluid. In the present paper, a self-excited global mode is found for a semi-infinite jet that is locally convectively unstable at every point.

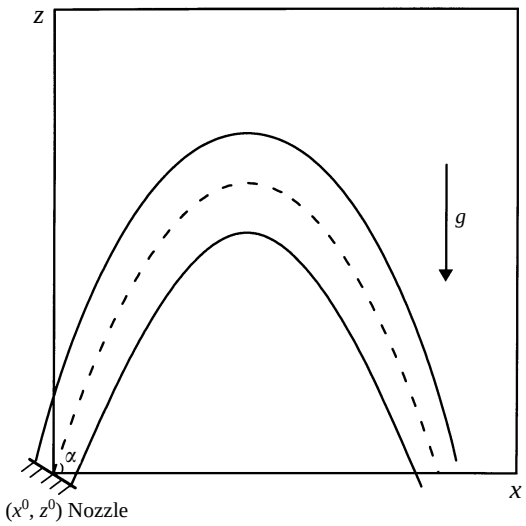


FIGURE 2. Flow geometry.

## 3. Instability of an inclined jet

### 3.1. *Formulation of the problem*

The flow under consideration is a jet of liquid that is incompressible and inviscid. The jet issues from a nozzle with a circular opening of radius $R_0$. The initial velocity $V_0$ is constant across the nozzle opening; its vector is inclined at an angle $\alpha$ to the horizontal, see figure 2. (Only the case $\alpha > 0$, which means the jet moves upward from the nozzle, is considered.) The influence of the surrounding medium is assumed to be negligible.

The length scale of the basic-flow streamwise development $L$ can be taken as the distance between the nozzle and the highest point of the jet trajectory; it can be expressed then as $L \sim V_0^2 g^{-1}$, in which $g$ is the acceleration due to gravity. The jet can be treated (locally) as an axially symmetric flow if

$$R_0 \ll \min(L, R_*), \tag{3.1}$$

in which $R_*$ is the typical radius of curvature of the jet centreline (Entov & Yarin 1984). If condition (3.1) is met, the basic flow is weakly inhomogeneous, since the typical wavelength of the local capillary instability is of order $R_0$. If the Froude number is introduced as $Fr = V_0 (gR_0)^{-1}$, condition (3.1) leads to

$$Fr \gg 1, \tag{3.2}$$

which indicates that the inertial forces dominate the gravity forces.

In the simplest approximation, the basic flow is assumed not to be affected by the capillary forces. Then, the jet centreline is similar to the trajectory of a stone thrown at an angle to the horizon (Tuck 1976), i.e.

$$z - z^0 = \tan(\alpha)\left(x - x^0\right) - \frac{\left(x - x^0\right)^2}{2Fr^2 \cos^2(\alpha)},$$

in which the horizontal and vertical coordinates $x$ and $z$ are made dimensionless by $R_0$, and the nozzle position is $\left(x^0, z^0\right)$. If the basic axial velocity is constant over each

cross-section, the velocity and radius in the dimensionless form are given by

$$V(X) = \left[1 - 2\tan(\alpha)\left(X - X^0\right) + \frac{\left(X - X^0\right)^2}{\cos^2(\alpha)}\right]^{1/2},$$

$$R(X) = [V(X)]^{-1/2},$$

in which the slow coordinate is $X = Fr^{-2}x$. Condition (3.2) is then replaced by

$$Fr \gg \cos^{-5/4}(\alpha). \tag{3.3}$$

If the viscous effects are taken into account, the basic flow can be calculated numerically (Goodwin & Schowalter 1994).

In contrast to the basic flow, the disturbances are assumed not to be affected by the gravity force. The local dispersion relation for axially symmetric disturbances can be represented in the following form:

$$\left(\omega\frac{R}{V} - G\right)^2 = We\frac{G\left(G^2-1\right)I_1(G)}{I_0(G)}, \tag{3.4}$$

in which

$$G(k, X) \equiv \text{sign}\left[\text{Re}(k)\right] kR(X), \tag{3.5}$$

$\omega$ and $k$ are made dimensionless by $R_0$ and $V_0$, and $I_0(G)$ and $I_1(G)$ are the modified Bessel functions. The local Weber number is introduced as

$$We(X) \equiv \frac{We_0}{R(X)V^2(X)},$$

in which $We_0 \equiv \sigma\left(\rho R_0 V_0^2\right)^{-1}$ is the Weber number at the nozzle; $\sigma$ and $\rho$ are the surface tension coefficient and the mass density of the liquid.

Equation (3.4) is a generalization of the famous dispersion relation of Rayleigh (1878) to the case of a spatially developing basic flow. Equation (3.5) implies that the dispersion relation is symmetric about the imaginary $k$-axis, so that one need consider only the half-plane $\text{Re}(k) > 0$. (The origin in the complex $k$-plane is a double branch point with two branch cuts along the positive and negative imaginary $k$ half-axes.)

The dispersion relation yields two branches of the local frequency

$$\omega = \frac{V}{R}\left\{G \pm \left[We\frac{G\left(G^2-1\right)I_1(G)}{I_0(G)}\right]^{1/2}\right\}.$$

For real $X$ and real $k > 0$, only one of the branches is 'temporally unstable', i.e. has values with positive imaginary parts. The region of unstable local wavenumbers is a single interval $0 < k < k^*(X)$, in which $k^*(X) \equiv R^{-1}(X)$ is a branch point of the local frequency.

In contrast to the frequency, the local wavenumber cannot be explicitly expressed from the dispersion relation. However, one can show that it has an infinite number of branches (Keller *et al.* 1973; Yakubenko 1997).

Dispersion relation (3.4) leads to the local absolute instability condition

$$We > We_{abs}. \tag{3.6}$$

In the general case, $We_{abs}$ depends on the shape of the profile of the mean axial velocity. For the present case of the uniform profile, $We_{abs} \approx 0.32$ (Leib & Goldstein 1986*a*; Monkewitz *et al.* 1988).

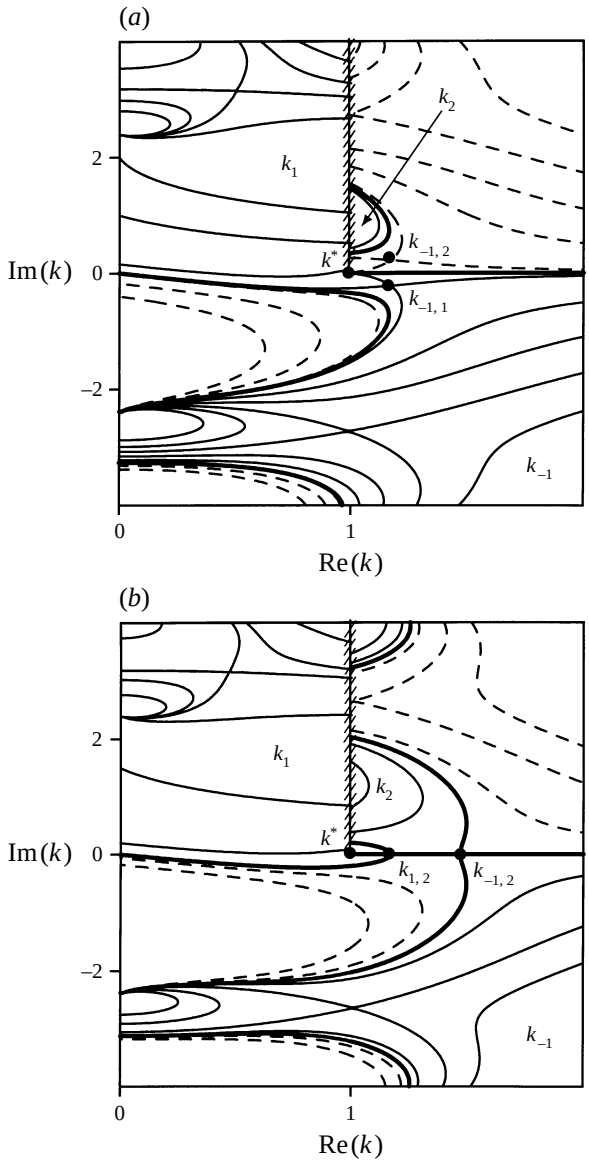


FIGURE 3. Typical contour plot of Im $[\omega(k)]$ in the cases of (*a*) local absolute instability ($We = 0.4$) and (*b*) local convective instability ($We = 0.3$). The solid, dashed, and bold lines are for positive, negative and zero values of Im $[\omega(k)]$, respectively. The branch cut is shown by the hatched line. The domains marked by $k_m$ correspond to different branches of the wavenumber for large Im $(\omega) > 0$.

### 3.2. *Global stability analysis*

The local Weber number reaches the maximum $We_0 \cos^{-3/2}(\alpha)$ at the highest point of the jet trajectory

$$X^{max} = X^0 + \sin(\alpha)\cos(\alpha).$$

Thus, the flow has no region of local absolute instability if

$$We_0 < We_{abs} \cos^{3/2}(\alpha). \tag{3.7}$$

Only this case is analysed in the present paper.

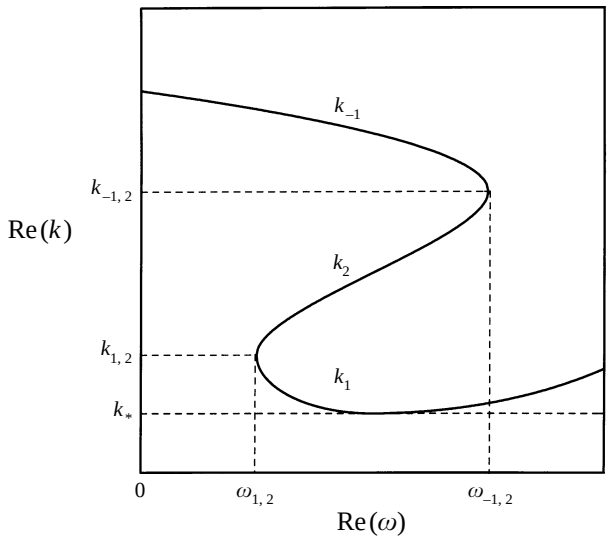


FIGURE 4. Typical local dispersion curve for real $X$. The parts of the curve corresponding to different branches of the wavenumber are marked by $k_m$.

A typical contour plot of $\mathrm{Im}\,[\omega(k, X)]$ on the complex $k$-plane is shown in figures 3($a$) and 3($b$) for the cases of local absolute and convective instability, respectively. Two saddle points determine the type of instability. The saddle points correspond on the complex $\omega$-plane to the branch points of three branches of the local wavenumber: $k_1(\omega, X)$, $k_2(\omega, X)$, and $k_{-1}(\omega, X)$. For large $\mathrm{Im}(\omega) > 0$, one has $\mathrm{Im}\,[k_1(\omega, X)] > 0$, $\mathrm{Im}\,[k_2(\omega, X)] > 0$, and $\mathrm{Im}\,[k_{-1}(\omega, X)] < 0$. Thus, the waves $K_1$ and $K_2$ propagate to the right, i.e. downstream, and the wave $K_{-1}$ propagates to the left, i.e. upstream. Note that for $\mathrm{Im}(\omega) > 0$, only $k_1(\omega, X)$ can have values with imaginary parts of different signs. Hence, only the wave $K_1$ can be spatially amplified in its direction of propagation for $\mathrm{Im}(\omega) > 0$.

The boundary conditions at the nozzle are assumed to be such that one can find the amplitude of every outgoing wave from the given amplitudes of the incoming waves. Additionally, no disturbance is assumed to come upstream from infinity.

For a real value of $X$, the typical dispersion curve $\mathrm{Re}\,[k_m(\omega, X)]$ vs. $\mathrm{Re}(\omega)$ is shown in figure 4. As $X$ increases from $X^0$ to $X^{max}$, both local absolute frequencies $\omega_{1,2}(X)$ and $\omega_{-1,2}(X)$ decrease. For $X > X^{max}$, the situation is symmetric. For any real $X$, one has

$$0 < \omega_{1,2}(X) < \omega_{-1,2}(X),$$

$$k^*(X) < k_{1,2}(X) < k_{-1,2}(X).$$

For any real frequency $\omega$ such that

$$\omega_{-1,2}(X^{max}) < \omega < \omega_{1,2}\left(X^0\right),$$

two pairs of turning points $X_{1,2}(\omega)$, $X_{-1,2}(\omega)$ and $\tilde{X}_{1,2}(\omega)$, $\tilde{X}_{-1,2}(\omega)$ are located at the real $X$-axis symmetrically around $X = X^{max}$. Additionally, two turning points $X_{-1,1}(\omega)$ and $\tilde{X}_{-1,1}(\omega)$ are located in the complex $X$-plane symmetrically around $X = X^{max}$. Three sets of the corresponding Stokes lines are shown in figure 5.

For $\mathrm{Im}(\omega) > 0$, the turning points move from the real $X$-axis into the complex plane. For sufficiently small $\mathrm{Im}(\omega) > 0$, the corresponding Stokes and anti-Stokes

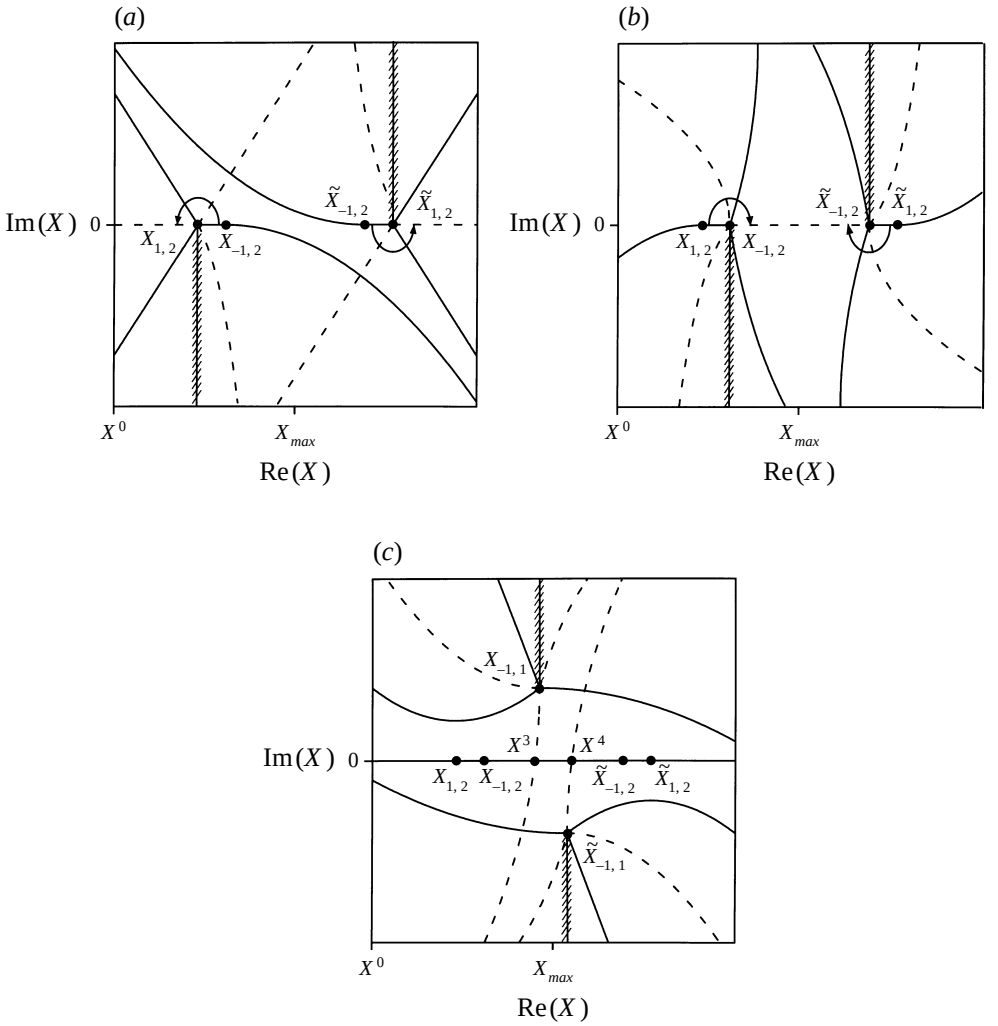


FIGURE 5. The solid and dashed lines sketch the Stokes and anti-Stokes lines for $\mathrm{Im}(\omega) = 0$, which correspond to the branches: (*a*) $K_1$ and $K_2$, (*b*) $K_{-1}$ and $K_2$, and (*c*) $K_{-1}$ and $K_1$. The branch cuts are shown by the hatched lines. The arrows show the directions in which the approximations are continued.

lines are similar to that shown in figure 6. Thus, the real $X$-axis crosses six anti-Stokes lines at the points $X^1, ..., X^6$. For $\mathrm{Im}(\omega) = 0$, the points $X^1$, $X^2$, $X^5$, and $X^6$ coincide with the turning points $X_{1,2}$, $X_{-1,2}$, $\tilde{X}_{-1,2}$ and $\tilde{X}_{1,2}$, respectively. In the following treatment, we assume that the structure of the Stokes and anti-Stoked lines is never topologically changed with respect to both the real $X$-axis and the position of the origin $X^0$.

Note that the transition from $\mathrm{Im}(\omega) = 0$ to $\mathrm{Im}(\omega) > 0$ changes the line's structure. Thus, for $\mathrm{Im}(\omega) = 0$, there is the anti-Stokes line that connects the turning points $X_{-1,2}$ and $\tilde{X}_{-1,2}$ (figure 5*b*). For stability analysis, we need to investigate only the case $\mathrm{Im}(\omega) > 0$. Moreover, we assume that the turning points are sufficiently far from each other, and the Stokes relations can be applied independently at each turning point.

The global mode is approximated by the following linear combinations of three

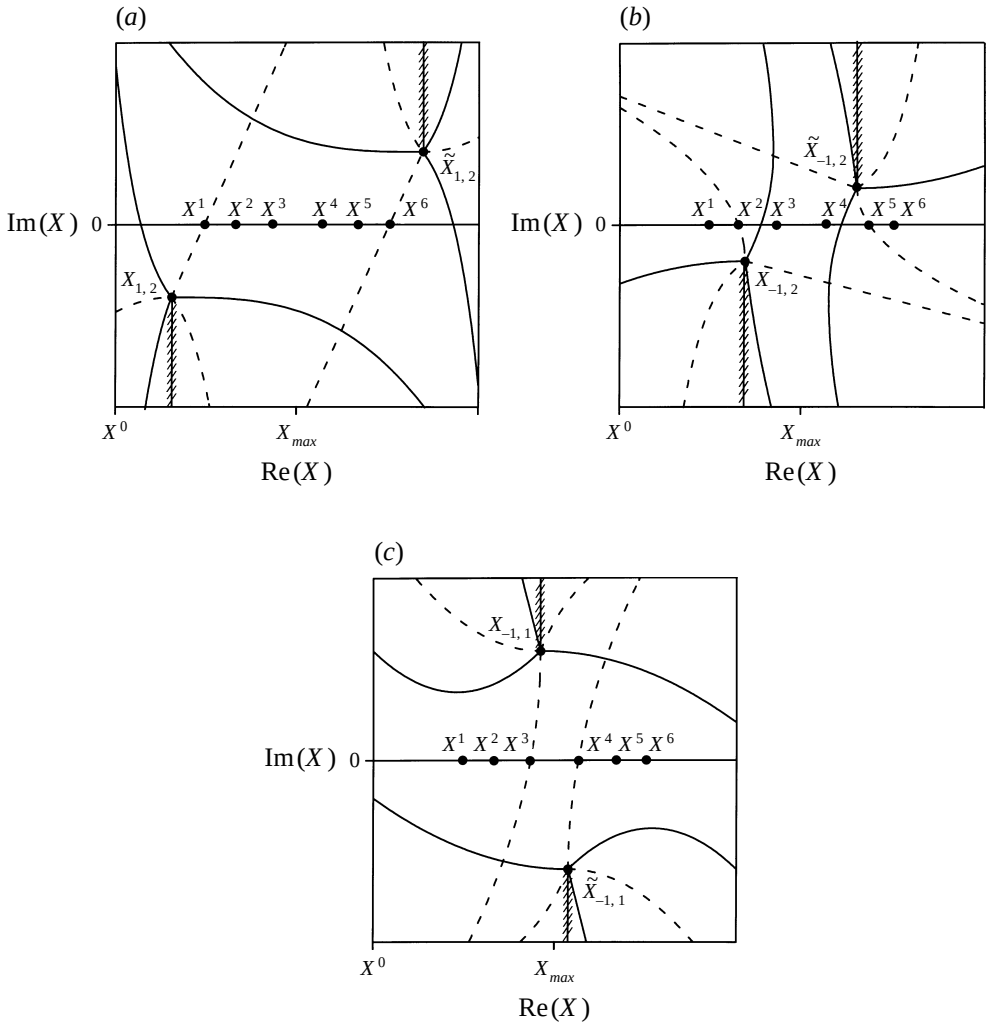


FIGURE 6. The solid and dashed lines sketch the Stokes and anti-Stokes lines for $\mathrm{Im}(\omega) > 0$, which correspond to the branches: (*a*) $K_1$ and $K_2$, (*b*) $K_{-1}$ and $K_2$, and (*c*) $K_{-1}$ and $K_1$. The branch cuts are shown by the hatched lines.

elementary waves $K_1$, $K_2$, and $K_{-1}$:

$$C_1^p K_2^p + C_2^p K_2^p + C_{-1}^q K_{-1}^q$$

at $[X^p, X^q]$, in which $p = 0, \ldots, 6$ and $q = 1, \ldots, 6, +\infty$.

The boundary conditions at the nozzle ($X = X^0$) can be expressed in the following form:

$$C_1^0 = P_{-1,1}^0 Q_{-1}^{1,0} C_{-1}^1, \tag{3.8}$$

$$C_2^0 = P_{-1,2}^0 Q_{-1}^{1,0} C_{-1}^1. \tag{3.9}$$

The conversion coefficients $P_{-1,1}^0$ and $P_{-1,2}^0$ are assumed to be of order unity.

For $\omega_{-1,2}(X^{max}) < \mathrm{Re}(\omega) < \omega_{1,2}(X^0)$, typical plots of $\mathrm{Im}[k_m(\omega, X)]$ vs. $\mathrm{Re}(X)$ are shown in figures 7(*a*) and 7(*b*) for the cases $\mathrm{Im}(\omega) = 0$ and $\mathrm{Im}(\omega) > 0$, respectively.

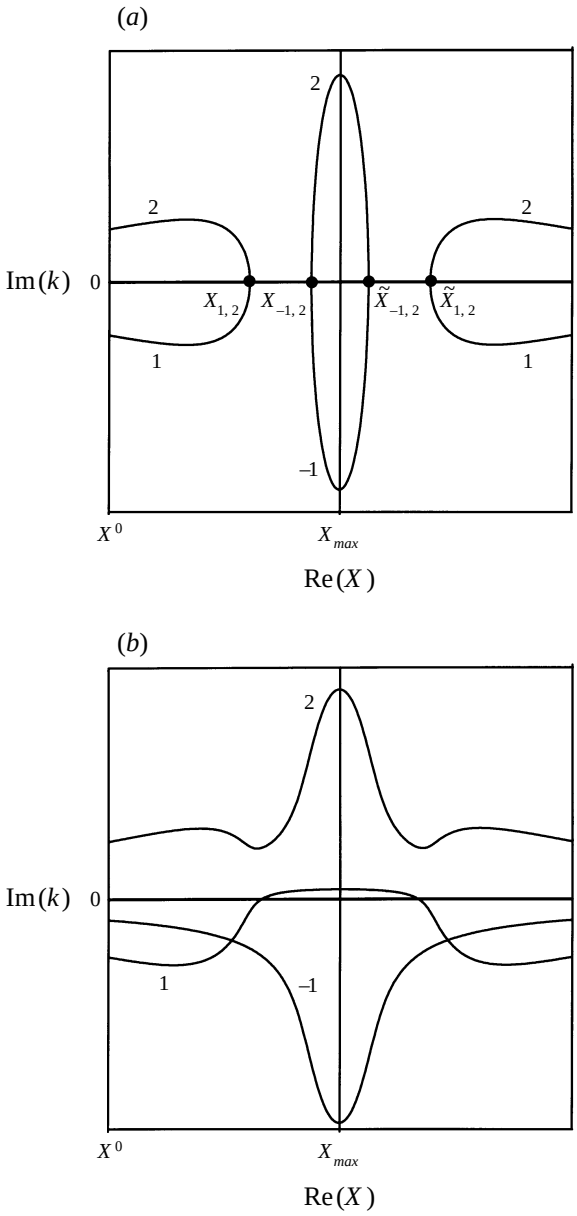


FIGURE 7. Typical plot of $\mathrm{Im}\,[k_m(\omega, X)]$ vs. real $X$ for the case of (*a*) $\mathrm{Im}\,(\omega) = 0$; (*b*) $\mathrm{Im}\,(\omega) > 0$. Different branches of the wavenumber are marked by the value of $m$.

For each turning point, these plots help to establish which WKBJ solution is dominant in which of the corresponding Stokes sectors.

The Stokes relations give the following additional boundary conditions at $X = X^1$ :

$$Q_1^{0,1} C_1^0 = C_1^1, \tag{3.10}$$

$$Q_2^{0,1} C_2^0 = C_2^1 + \mathrm{i} R_{1,2}^1 C_1^1, \tag{3.11}$$

$$C_{-1}^1 = Q_{-1}^{2,1} C_{-1}^2; \tag{3.12}$$

$X = X^2$ :

$$C_1^2 = Q_1^{1,2} C_1^1, \tag{3.13}$$

$$C_2^2 = Q_2^{1,2} C_2^1, \tag{3.14}$$

$$Q_{-1}^{3,2} C_{-1}^3 = C_{-1}^2 - \mathrm{i} R_{2,-1}^2 Q_2^{1,2} C_2^1; \tag{3.15}$$

$X = X^5$ :

$$C_1^5 = Q_1^{4,5} C_1^4, \tag{3.16}$$

$$Q_2^{4,5} C_2^4 = C_2^5 - \mathrm{i} R_{-1,2}^5 Q_{-1}^{6,5} C_{-1}^6, \tag{3.17}$$

$$C_{-1}^5 = Q_{-1}^{6,5} C_{-1}^6; \tag{3.18}$$

$X = X^6$ :

$$C_1^6 = Q_1^{5,6} C_1^5 + \mathrm{i} R_{2,1}^6 Q_2^{5,6} C_2^5, \tag{3.19}$$

$$C_2^6 = Q_2^{5,6} C_2^5, \tag{3.20}$$

$$C_{-1}^6 = Q_{-1}^{+\infty,6} C_1^{+\infty}, \tag{3.21}$$

in which $R_{1,2}^1$, $R_{2,-1}^2$, $R_{-1,2}^5$ and $R_{2,1}^6$ are given by (2.6) with the upper integration limit taken as $X_{1,2}$, $X_{-1,2}$, $\tilde{X}_{-1,2}$ and $\tilde{X}_{1,2}$, respectively.

The directions in which the solutions are continued around the turning points are shown in figure 5. Equations (3.10)–(3.21) are written in the form that serves to emphasize these directions. Note that for $\mathrm{Im}\,(\omega) = 0$, an extra relation would be required at the anti-Stokes line that connects the turning points $X_{-1,2}$ and $\tilde{X}_{-1,2}$.

Since no disturbance comes upstream from infinity, one must have $C_{-1}^{+\infty} = 0$. Equations (3.21) and (3.18) then give

$$C_{-1}^5 = C_{-1}^6 = 0,$$

and (3.17) becomes

$$C_2^5 = Q_2^{4,5} C_2^4. \tag{3.22}$$

Owing to the structure of the Stokes and anti-Stokes lines, the wave $K_2$ does not interact with the other waves in the interval $\left(X^3, X^4\right)$. Therefore,

$$C_2^4 = Q_2^{3,4} C_2^3. \tag{3.23}$$

However, the waves $K_1$ and $K_{-1}$ may interact. Strictly speaking, the matching of the WKBJ solutions around a turning point must be always started from a narrow sector that contains the Stokes line. Therefore, the interaction of $K_1$ and $K_{-1}$ cannot be accounted for in a simple way similar to (3.10)–(3.21).

Fortunately, the structure of the corresponding Stokes and anti-Stokes lines resembles the problem of particle scattering from the *underdense potential barrier* (see, e.g. Heading 1962, §5.3). Thus, the interaction is weakening exponentially with the distance between the real $X$-axis and the turning point $X_{-1,1}$ (or $\tilde{X}_{-1,1}$). Since for $\mathrm{Im}\,(\omega) \geqslant 0$, the turning points $X_{-1,1}$ and $\tilde{X}_{-1,1}$ are located relatively far away from the real axis, we neglect the interaction and simply write

$$C_1^5 = Q_1^{2,5} C_1^2, \quad C_{-1}^3 = Q_{-1}^{5,3} C_{-1}^5 = 0. \tag{3.24}$$

Then, (3.15) simplifies to

$$0 = C_{-1}^2 - \mathrm{i} R_{2,-1}^2 Q_2^{1,2} C_2^1. \tag{3.25}$$

Equations (3.8)–(3.12) and (3.25) form a system of six homogeneous linear algebraic equations for $C_1^0$, $C_2^0$, $C_1^1$, $C_2^1$, $C_{-1}^1$, and $C_{-1}^2$. The system can have a non-trivial solution only if its determinant is zero, which gives the following equation for the global frequencies:

$$\Delta(\omega) \equiv Q_1^{0,1} R_{1,2}^1 Q_2^{1,2} R_{2,-1}^2 Q_{-1}^{2,0} P_{-1,1}^0 + \mathrm{i} Q_2^{0,1} Q_2^{1,2} R_{2,-1}^2 Q_{-1}^{2,0} P_{-1,2}^0 = 1. \tag{3.26}$$

If $0 < \mathrm{Im}(\omega) \ll 1$, then $R_{2,-1}^2$, $R_{1,2}^1$, $Q_{-1}^{2,0}$, and $Q_2^{1,2}$ are of unit order of magnitude, while $\left|Q_1^{0,1}\right| \gg 1$ and $\left|Q_2^{0,1}\right| \ll 1$. Therefore, $|\Delta(\omega)| \gg 1$ and (3.26) has no solution.

As $\mathrm{Im}(\omega)$ increases, all $R_{2,-1}^2$, $R_{1,2}^1$, $Q_{-1}^{2,0}$, $Q_2^{1,2}$, $Q_1^{0,1}$, and $Q_2^{0,1}$ decrease in magnitude. (For $\mathrm{Im}(\omega) \gg 1$, every wave is spatially damped in its direction of propagation, so that every $\left|Q_m^{i,j}\right| \ll 1$.) Then, one can easily choose $\mathrm{Im}(\omega) > 0$ such that (3.26) is satisfied.

Moreover, the amplification of the wave $K_1$ at $\left[X^0, X^1\right]$ is

$$\left|Q_1^{0,1}\right| \sim \exp\left(X^1 - X^0\right).$$

Therefore, it decreases if $X^1$ gets close to the orifice $X^0$, which occurs if $\mathrm{Re}(\omega)$ approaches $\omega_{1,2}\left(X^0\right)$. Since the required structure of the Stokes and anti-Stokes lines is kept only for sufficiently small $\mathrm{Im}(\omega) > 0$, one can expect global frequencies with $\mathrm{Re}(\omega)$ close to $\omega_{1,2}\left(X^0\right)$.

The unstable global mode is constructed above for frequencies such that

$$\omega_{-1,2}\left(X^{max}\right) < \mathrm{Re}(\omega) < \omega_{1,2}\left(X^0\right).$$

The sufficient condition of global instability can be expressed as the following implicit relation between $\alpha$ and $We_0$:

$$\omega_{-1,2}\left[X^0 + \sin(\alpha)\cos(\alpha), We_0\right] < \omega_{1,2}\left(X^0, We_0\right). \tag{3.27}$$

In figure 8, the domain of global instability is represented on the $(\alpha, We_0)$-plane. The presence of a local absolute instability region is not necessary for the flow to be globally unstable. (Although the result is shown for $\alpha$ from 0 to $\pi/2$, the values very close to $\pi/2$ are inappropriate because of (3.3).)

For the global frequencies, one must have

$$Q_1^{0,1} R_{1,2}^1 Q_2^{1,2} R_{2,-1}^2 Q_{-1}^{2,0} P_{-1,1}^0 \approx 1,$$

which implies a sequence of three wave: $K_1$ at $\left[X^0, X^1\right]$, $K_2$ at $\left[X^1, X^2\right]$, and $K_{-1}$ at $\left[X^2, X^0\right]$. The waves are consequently converted from one into the other, and the total product of their space amplification coefficients and their conversion coefficients is of order unity. Thus, the result is of agreement with the general criterion of global instability (2.7).

The second term in $\Delta(\omega)$ can be rewritten as $\mathrm{i} Q_2^{0,2} R_{2,-1}^2 Q_{-1}^{2,0} P_{-1,2}^0$. It corresponds to a sequence of two waves: $K_2$ at $\left[X^0, X^2\right]$ and $K_{-1}$ at $\left[X^2, X^0\right]$. However, this sequence never evolves into a global mode, since the required amplitude balance cannot be achieved.

If $C_1^1$ and $C_2^1$ are found, equations (3.13), (3.14), (3.16), (3.19), (3.20), and (3.22)–(3.24) straightforwardly give

$$C_2^6 = Q_2^{1,6} C_2^1,$$

$$C_1^6 = Q_1^{1,6} C_1^1 + \mathrm{i} R_{2,1}^6 Q_2^{1,6} C_2^1.$$

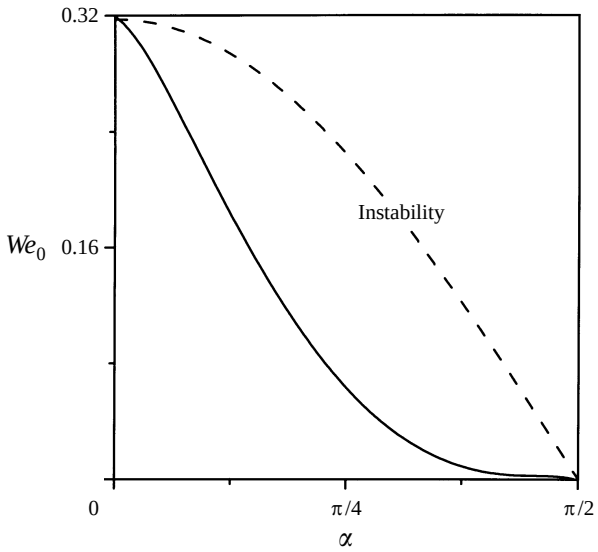


FIGURE 8. The jet is globally unstable for the domain above the solid line; the local instability is convective for the domain below the dashed line.

Note that the wave $K_1$ spatially grows downstream from $X = X^6$. As its amplitude becomes finite, the disturbance develops nonlinearly and causes the jet to break up into drops far downstream from the nozzle. No disturbance is assumed to come back upstream from that 'nonlinear zone'.

Finally, the eigenvalue relation (3.26) can be rewritten as

$$\Delta(\omega) = R^0_{1,2}R^0_{2,-1}P^0_{-1,1} + \mathrm{i}R^0_{2,-1}P^0_{-1,2} = 1. \tag{3.28}$$

Thus, $\Delta(\omega)$ is can be exponentially large or small depending on the position of the orifice $X^0$ with respect to the turning points and Stokes lines. Although (3.28) looks simpler than (3.26), the latter allows a more transparent physical interpretation in terms of the wave propagation.

### 3.3. *Experimental observation of the instability*

A simple experiment was performed in order to observe the global instability. A jet of water issued from a nozzle that was located on an inclined sidewall of a large tank. The upper side of the tank was open to the atmosphere so that the water level in the tank dropped slowly. Thus, the basic flow was quasi-stationary. The initial water level in the tank was such that the Weber number at the nozzle $We_0$ was very small so that the flow was stable (figure 9*a*).

As the water level decreased, $We_0$ reached the critical value, and the axially symmetric global mode began to grow (figure 9*b*). When its amplitude had increased sufficiently, the disturbance started to evolve nonlinearly. Then, besides the axially symmetric mode, torsional and bending disturbances were excited (figure 9*c*). Further nonlinear evolution of the disturbances caused the flow to oscillate quasi-periodically with a finite amplitude. In all the cases shown in figure 9(*a–c*), the estimated maximum value of the local Weber number is less than 0.25. According to the theory, the local instability can be absolute only for local Weber numbers above 0.32. Thus,

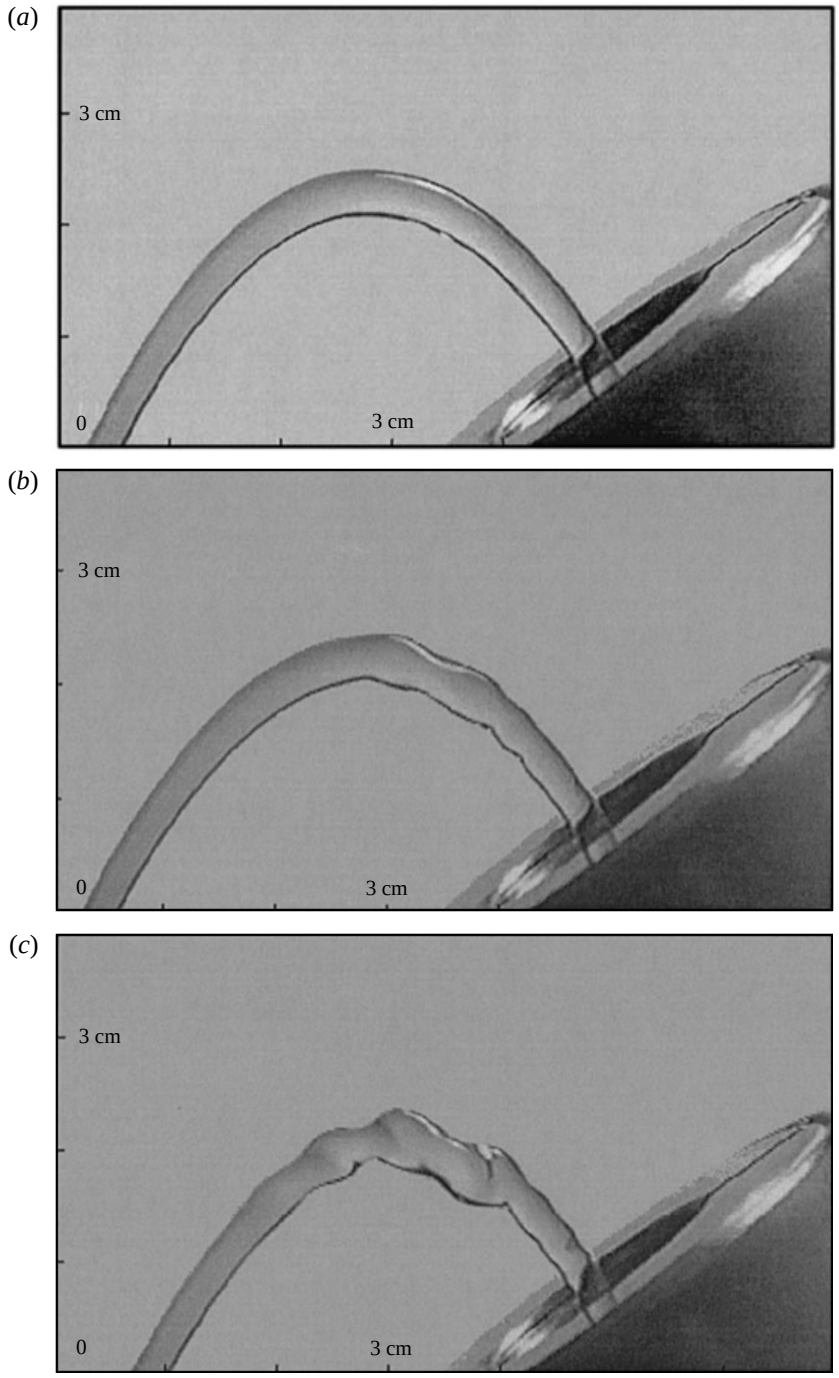


FIGURE 9. Experimental observation of instability of an inclined jet of water: (*a*) stable flow; (*b*) axially symmetric global mode starts to grow; (*c*) developed instability. In all three cases, $R_0 = 1.5$ mm and $\alpha = \pi/3$.

the experiment has confirmed the theoretical conclusion that a jet that is locally convectively unstable can sustain a self-excited global mode.

In real jets, the axial velocity profile often diverges from uniform near the nozzle, yet it approaches the uniform state farther downstream. Such relaxation of the velocity profile can be modelled by a sequence of parabolic Poiseuille-type profiles. The critical value of the local Weber number, above which the instability is absolute, is greater for such profiles than for the uniform one (Leib & Goldstein 1986*a*). Thus, one can say that a jet with the relaxing profile is locally 'more' convectively unstable. The effect can change the range of global frequencies, but it does not eliminate them.

## 4. Conclusions

A global linear stability analysis is performed for an inviscid circular jet that issues from a nozzle at an angle to the gravitational field. A self-excited global mode is found for the flow that is locally convectively unstable at every point. The global mode is based on a combination of three elementary WKBJ solutions. The nozzle plays an essential role in the mode formation.

A simple experiment proves the existence of the mode and shows that it can evolve into a wave of finite amplitude that is localized in space near the nozzle.

The author thanks G. A. Shugai, A. G. Kulikovskii, I. S. Shikina and, especially, S. Le Dizès for numerous comments and discussions.

## Appendix A. How to locate the Stokes lines

First, all turning points must be found. They are given by the simultaneous solutions of the dispersion relation and its $k$-derivative, i.e.

$$D(k,\omega,X)=0, \quad D_k(k,\omega,X)=0,$$

in which $\omega$ is a parameter.

The Stokes lines that emerge from the turning point $X_{m,n}$ are defined by the relation

$$G(X)\equiv \operatorname{Im}[F(X)]=0$$

with

$$F(X)\equiv \int_{X_{m,n}}^{X}[k_m(\omega,\xi)-k_n(\omega,\xi)]\,\mathrm{d}\xi,$$

in which $\omega$ is a parameter. If $X=X_r+\mathrm{i}X_i$, then $(-\partial G/\partial X_i, \partial G/\partial X_r)$ is a vector field that is tangential to the curves $G(X)=\text{const}$. Since $F(X)$ is an analytic function,

$$\frac{\partial G}{\partial X_i}=\frac{\partial}{\partial X_r}\operatorname{Re}(F)=\frac{\partial}{\partial X_i}\operatorname{Im}(F).$$

Hence, the curves $G(X)=\text{const}$ are integral curves of the differential equation

$$\frac{\mathrm{d}X_i}{\mathrm{d}X_r}=-\frac{\partial}{\partial X_r}\operatorname{Im}(F)\Big/\frac{\partial}{\partial X_r}\operatorname{Re}(F).$$

Since

$$\begin{aligned}\frac{\partial}{\partial X_r}[\operatorname{Re}(F)+\mathrm{i}\operatorname{Im}(F)]&=\frac{\partial F}{\partial X_r}=\frac{\partial F}{\partial X}\\&=\operatorname{Re}[k_m(\omega,X)-k_n(\omega,X)]+\mathrm{i}\operatorname{Im}[k_m(\omega,X)-k_n(\omega,X)],\end{aligned}$$

the differential equation can be rewritten as

$$\frac{\mathrm{d}X_i}{\mathrm{d}X_r} = -\frac{\mathrm{Im}\,[k_m(\omega, X) - k_n(\omega, X)]}{\mathrm{Re}\,[k_m(\omega, X) - k_n(\omega, X)]}.$$

If $k_j(\omega, X)$ cannot be explicitly expressed from the dispersion relation, it can be calculated from the following differential equation:

$$\frac{\mathrm{d}k_j}{\mathrm{d}X} = -\frac{D_X(k_j, \omega, X)}{D_k(k_j, \omega, X)},$$

in which the subscripts $k$ and $X$ stand for $k$- and $X$-derivatives, respectively, and $\omega$ is a parameter. Finally, one has a system of three ordinary differential equations

$$\frac{\mathrm{d}X_i}{\mathrm{d}X_r} = -\frac{\mathrm{Im}\,(k_m - k_n)}{\mathrm{Re}\,(k_m - k_n)},$$

$$\frac{\mathrm{d}k_m}{\mathrm{d}X_r} = -\frac{D_X(k_m, \omega, X_r + \mathrm{i}X_i)}{D_k(k_m, \omega, X_r + \mathrm{i}X_i)},$$

$$\frac{\mathrm{d}k_n}{\mathrm{d}X_r} = -\frac{D_X(k_n, \omega, X_r + \mathrm{i}X_i)}{D_k(k_n, \omega, X_r + \mathrm{i}X_i)},$$

in which $\omega$ is a parameter. By the theorem of uniqueness, exactly one curve $G(X) =$ const passes through each point except the turning points $X_{m,n}$.

If $X_{m,n}$ is a turning point of order $s$, it is a common point of $s + 2$ distinct Stokes lines. Neighbouring lines meet at the angle $2\pi/(s+2)$ (see e.g. Wasow 1985). The rule helps to localize the Stokes lines after the turning points are found and the contour plot of $G(X)$ is performed. It should be mentioned that the turning points are branch points of $G(X)$. Therefore, the branch cuts must be taken into account.

Finally, the sets of Stokes lines that correspond to different pairs of the branches $k_j(\omega, X)$ are completely independent. The lines from different sets may intersect at any point and even coincide. Hence, the routine described above can be performed independently for each set.

## REFERENCES


Akhiezer, A. I. & Polovin, R. V. 1971 Criteria for wave growth. *Sov. Phys. Usp.* **14**, 278–285.

Ashgriz, N. & Mashayek, F. 1995 Temporal analysis of capillary jetbreakup. *J. Fluid Mech.* **291**, 163–190.

Bers, A. 1983 Space-time evolution of plasma instabilities—absolute and convective. In *Handbook of Plasma Physics* (ed. M. N. Rosenbluth & R. Z. Sagdeev), vol. 1, ch. 3.2. North-Holland.

Bogy, D. B. 1979 Drop formation in a circular liquid jet. *Ann. Rev. Fluid Mech.* **11**, 207–228.

Chomaz, J. M., Huerre, P. & Redekopp, L. G. 1988 Bifurcations to local and global modes in spatially-developing flows. *Phys. Rev. Lett.* **60**, 25–28.

Chomaz, J. M., Huerre, P. & Redekopp, L. G. 1991 A frequency selection criterion in spatially developing flows. *Stud. Appl. Maths* **84**, 119–144.

Crighton, D. G. & Gaster, M. 1976 Stability of slowly diverging jet flow. *J. Fluid Mech.* **77**, 397–413.

Dnestrovskii, Y. N. & Kostomarov, D. P. 1964 On the asymptotic eigenvalues for non-self-adjoint boundary-value problems. *Comput. Math. Math. Phys.* **4**, 267–275.

Drazin, P. G. 1974 Kelvin-Helmholtz instability of a slowly varying flow. *J. Fluid Mech.* **65**, 781–797.

Entov, V. M. & Yarin, A. L 1984 The dynamics of thin liquid jets in air. *J. Fluid Mech.* **140**, 91–111.

Goodwin, R. T. & Schowalter, W. R. 1994 Arbitrarily oriented capillary-viscous planar jets in the presence of gravity. *Phys. Fluids* **7**, 954–963.

Heading, J. 1962 *An Introduction to Phase-Integral Methods.* Methuen.

Huerre, P. & Monkewitz, P. A. 1990 Local and global instabilities in spatially developing flows. *Ann. Rev. Fluid Mech.* **22**, 473–537.

Hunt, R. E. & Crighton, D. G. 1991 Instability of flows in spatially developing media. *Proc. R. Soc. Lond.* A **435**, 109–128.

Iordanskii, S. V. 1988 Stability of nonhomogeneous states and path integrals. *Sov. Phys. JETP* **68**, 1398–1402.

Keller, J. B., Rubinow, S. I. & Tu, Y. O. 1973 Spatial instability of a jet. *Phys. Fluids* **16**, 2052–2055.

Krall, N. A. & Rosenbluth, M. N. 1963 Low-frequency stability of nonuniform plasmas. *Phys. Fluids* **6**, 254–265.

Kulikovskii, A. G. 1966 On the stability of homogeneous states. *J. Appl. Math. Mech.* **30**, 180–187.

Kulikovskii, A. G. 1985 On the stability conditions for stationary states or flows in regions extended in one direction. *J. Appl. Math. Mech.* **49**, 316–321.

Kulikovskii, A. G. 1993 On the stability loss of weakly non-uniform flows in extended regions. The formation of transverse oscillations of a tube conveying a fluid. *J. Appl. Math. Mech.* **57**, 851–856.

Le Dizès, S. 1996 Global modes in falling capillary jets. In *Proc. EUROMECH Colloquium* 355. Paliseau.

Le Dizès, S., Huerre, P., Chomaz, J.-M. & Monkewitz, P. A. 1996 Linear global modes in spatially developing media. *Phil. Trans. R. Soc. Lond.* A **354**, 169–212.

Leib, S. J. & Goldstein, M. E. 1986*a* The generation of capillary instability on a liquid jet. *J. Fluid Mech.* **168**, 479–500.

Leib, S. J. & Goldstein, M. E. 1986*b* Convective and absolute instability of a liquid jet. *Phys. Fluids* **29**, 952–954.

Lifshitz, E. M. & Pitaevskii, L. P. 1981 *Physical Kinetics.* ch. 6. Pergamon.

Lin, S. P. & Lian, Z. W. 1989 Absolute instability of a liquid jet in a gas. *Phys. Fluids* A **1**, 490–493.

Meyer, R. E. 1989 A simple explanation of the Stokes phenomenon. *SIAM Rev.* **31**, 435–445.

Monkewitz, P. A. 1990 The role of absolute and convective instability in predicting the behavior of fluid systems. *Eur. J. Mech.* B/*Fluids* **9**, 395–413.

Monkewitz, P. A., Davis, J., Bojorquez, B. & Yu, M. H. 1988 The breakup of a liquid jet at high Weber number. *Bull. Am. Phys. Soc.* **33**, 2273.

Monkewitz, P. A., Huerre, P. & Chomaz, J. M. 1993 Global linear stability analysis of weakly non-parallel shear flows. *J. Fluid. Mech.* **251**, 1–20.

Monkewitz, P. A., Huerre, P. & Redekopp, L. G. 1987 Preferred modes in jets and global instabilities. *Bull. Am. Phys. Soc.* **32**, 2051.

Pierrehumbert, R. T. 1984 Local and global baroclinic instability of zonally varying flows. *J. Atmos. Sci.* **41**, 2141–2162.

Rayleigh, Lord 1878 On the instability of jets. *Proc. Lond. Math. Soc.* **10**, 4–13.

Silin, V. P. 1963 Oscillations of a weakly inhomogeneous plasma. *Sov. Phys. JETP* **17**, 857–864.

Stokes, G. G. 1857 On the discontinuity of arbitrary constants which appear in divergent developments. *Trans. Camb. Phil. Soc.* **9**, 166–187. Reprinted in *Mathematical and Physical Papers*, vol. 2, pp. 329–357, 1883. Cambridge University Press.

Tuck, E. O. 1976 The shape of free jets of water under gravity. *J. Fluid Mech.* **76**, 625–640.

Wasow, W. 1985 *Linear Turning Point Theory*. Springer.

Yakubenko, P. A. 1997 Capillary instability of an ideal jet of large but finite length. *Eur. J. Mech.* B/*Fluids* **16**, 39–47.